

ATOMISTIC SIMULATIONS OF CARBON NANOTUBES HETERO-JUNCTIONS

Antonio F. Ávila, aavila@netuno.lcc.ufmg.br

Maria Gabriela R. Carvalho, mariagabrielacarvalho@yahoo.com.br

José de Ávila Junior jose.avila@javila.net

Guilherme R.S. Lacerda

Universidade Federal de Minas Gerais, Department of Mechanical Engineering and Graduate Program on Mechanical Engineering (PPGMEC-UFMG), 6627 Antonio Carlos Avenue, Belo Horizonte, MG 31270-901, Brazil

Abstract. During carbon nanotubes synthesis a large amount of “defected” ones are generated. The purification process involves, in general, high costs. The market price of single walled carbon nanotubes (SWNT) with 99,999% purity is close to US\$500,00/gram. To be able to use these defective nanotubes as reinforcements for composites, their mechanical properties must be known. Considerable work has been done by Gates and his co-workers into the field of carbon nanotubes and composites reinforced by carbon nanotubes. However, the characterization of defective carbon nanotubes, also called hetero-junctions, is still an open question. Notice that hetero-junction properties can have large variations, as those are dependent on the SWNT configurations. The so called molecular mechanics model is employed to investigate two defects configurations, i.e. Dunlap and Sadoc, and their stress concentration regions are located. These regions are the ones with the highest probability of failure. The model is validated against data from literature on non-defective single walled carbon nanotubes with good agreement.

Keywords: single walled carbon nanotubes, hetero-junctions, molecular mechanics, nanotechnology

1. INTRODUCTION

As described by Saito and his co-workers (2005), carbon nanotube is a honeycomb lattice rolled into a cylinder. Carbon nanotubes (CNTs) have been the center of many researches due to their dimensions and remarkable electro-mechanical properties. In general, a CNT diameter has a nanometer size and its length can be more than 1 μ m. Such large aspect ratio (length/diameter) is appointed as one of the reasons for the CNTs notable properties. Consistent with Kalamkarov et al. (2006), single-walled nanotubes (SWNTs) have predicted specific strength around 600 times larger than steel. Another important issue of CNTs is their remarkable thermal and electrical properties. They are thermally stable up to 2800 C (in vacuum), reveal a thermal conductivity about twice as high as diamond, and may exhibit a capacity to carry electric current a thousand times better than copper wires.

CNT capabilities have been observed experimentally and verified by numerical simulations. Jin and Yuan (2003) and Yu et al. (2000) are among those researchers whom employed molecular dynamics for analyzing carbon nanotubes. The atomistic simulation approach was applied by Belystchko et al. (2002), Gates and co-workers (2005) while the nano-mechanics modeling was described by Liu et al. (2004) and Li and Chou (2003). Although carbon nanotubes have tremendous potential applications in a large variety of usages, e.g. aerospace industry, medical and electronic devices, there is no consensus about their exact mechanical properties. The experiments performed up to now have presented large variability due to the inherent complexity of manipulating these materials. Furthermore, the traditional molecular dynamics (MD) simulations are limited and computationally expensive.

In this paper, the concept of molecular structural mechanics described by Li and Chou (2003) and Tserpes and Papanikos (2005), and extended by Ávila and Lacerda (2008) is associated to the three-dimensional finite element model and later on employed to predict the mechanical properties of defective Single-Walled Carbon Nanotubes (SWNTs), also described as hetero-junctions. Numerical simulations considering the three major configurations (armchair, zigzag and chiral) are prepared for validation purposes. Furthermore, a parametric study on wall thickness, diameter and chirality effects on stiffness is also performed. Finally, the Sadoc and Dunlap hetero-junctions are simulated to be able to identify regions with the highest probability of failure.

2. LITERATURE REVIEW

According to Terrones (2003), in 1991 Iijima using a high resolution transmission electron microscope and electron diffraction, reported the existence of helical carbon microtubules (now called nanotubes) consisting of nested graphene tubules. This material was generated in an arc-discharge fullerene reactor (operating at low direct current). These concentric tubules exhibited interlayer spacing of approximately 3.4 Å, a value slightly greater than that of graphite (3.35 Å). Iijima (1991) associated this spacing difference to a combination of the graphene sheet curvature and weaker Van der Waals forces acting between the successive cylinders. Since this first report, the scientific community is investigating the nanotubes, mainly due to their fabulous properties. As stated by Natsuki et al. (2004), experimental methods for measuring the mechanical properties of CNTs are mainly based on the techniques of transmission electron

microscopy (TEM) and atomic force microscopy (AFM). They described the results obtained by Treacy and collaborators. for multi-walled carbon nanotubes (MWNT). According to them, by measuring thermal vibration using TEM, Treacy et al obtained a Young modulus of 1.8 ± 0.9 TPa. Natsuki and his co-workers (2004) also reported a slightly lower value of 1.28 ± 0.59 TPa with little dependence of nanotube diameter obtained by Wong et al. using the AFM tip to bend anchored MWNTs. A set of experiments performed by Yu and collaborators (2000) in MWNT lead to data ranging from 11 to 63 GPa and 0.27 to 0.95 TPa to tensile strength and Young's modulus, respectively.

The results obtained for single-walled carbon nanotubes (SWNTs) follow the same pattern. Krishnan et al. (1998) have reported a study on single-walled carbon nanotubes (SWNT) using the TEM technique. The SWNT had a diameter range of 1.0–1.5 nm, and the elastic modulus was measured to be the mean value of 1.30 ± 0.4 TPa. Yu et al. (2000) have also obtained the mechanical responses of SWNT bundles under tensile loading. The values of elastic modulus ranged from 0.32 to 1.47 TPa with a mean value of 1.02 TPa, and a tensile strength from 13 to 53 GPa. Lourie and Wagner (1998) obtained the axial Young's modulus for a series of temperatures by micro-Raman spectroscopy from measurements of cooling-induced compressive deformation of nanotubes embedded in an epoxy matrix.

At low temperature, ≈ 80 K, Lourie and Wagner (1998) got a 3.0 TPa axial Young's modulus for SWNT with an average radius of 0.7 nm, and 2.4 TPa for MWNTs with an average radius of 5–10 nm. Xiao et al. (2005), however, reported for SWNT the tensile modulus ranged from 0.27 to 3.6 TPa, while the ultimate strength varied from 11 to 200 GPa. With such variability on these results, Xiao and his colleagues concluded that CNT, single or multi-walled, elastic properties are highly dependent on its structure.

Due to the complexity in experimental characterization of nanotubes, computer simulation has been regarded as a powerful tool for modeling the properties of nanotubes. Wang et al. (2003) reported that MD formulations were probably the most popular method currently employed for nano-scale analysis, due to its availability of accurate interatomic potentials for a range of materials. However, a critical issue on MD simulations remains, i.e. temperature. The temperature induced high frequency molecular thermal vibration, on scale of 10^{15} Hz, makes difficult to estimate strains, even worst, limit the deformation calculations to nano-seconds. Liu et al. (2004) mentioned that in most applications nanoscale materials are used in association to other components that are larger, and have different response times, thus operating at different time and length scales. Furthermore, single scale methods such as *ab initio* quantum mechanical methods or molecular dynamics (MD) will have difficulty in analyzing such hybrid structures due to the limitations in terms of the time and length scales that each method is confined to. Yet, the length and time scales that can be probed using MD are still fairly limited. For the study of nanoscale mechanics and materials, Liu and collaborators suggested model up to a scale of several microns, consisting of billions of atoms, which is too large for MD simulations to-date. Hence, there is a need to develop multi-scale approaches for this class of problems.

The fundamental relations governing the geometry of CNT were described by Dresselhaus et al. (1995). They were able to explain the mathematical expression that relates the graphene sheet geometry in a honeycomb-like design and the carbon nanotubes three main configurations, i.e. chiral, zigzag and armchair. By doing it, they opened the possibility to CNT computer simulations. For Gates et al. (2003), the large majority of numerical and analytical approaches can be classified into two categories: the "bottom up" approach based on quantum/molecular mechanics including the classical molecular dynamics (MD), and the "top down" based on continuum mechanics. A third category, however, can be established; it is called multi-scale methods, where the continuum mechanics models are coupled to MD expressions. The Equivalent-Continuum Model described by Odegard and his colleagues (2002) successfully linked atomistic simulations of nano-structured materials to continuum models of the corresponding bulk material. In a series of papers, the NASA Langley Research Group headed by Gates (Odegard et al. 2005) developed numerical models for atomistic simulations coupling different approaches ranging from molecular dynamics to finite element and continuum mechanics with significant results. The so called molecular mechanics approach described by Gates et al. (2003) is the basis of this research. However, the atomistic simulations are focused into SWNTs with defects. These defects can be the ones described by Belytschko et al. (2002), where missing atoms lead to failure, or hetero-junctions. As illustrated by Mechor and Dobado (2004), hetero-junctions are generated when two CNTs are linked. There are two types of hetero-junctions, i.e. Dunlap and Sadoc as described in Figure 1. Each one of these hetero-junctions leads to unique stress concentration regions, and possible failure locations.

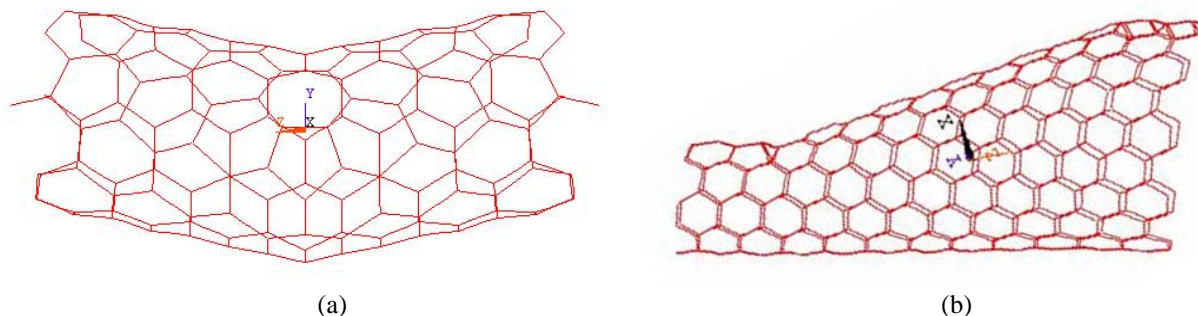


Figure 1. Typical defect geometry: (a)Dunlap e (b)Sadoc.

Li and Chou (2003) defined the multi-scale modeling technique as a combination of the atomistic molecular structural mechanics approach described by Li and Chou (2003) and the continuum finite element method. This approach was also implemented by Meo and Rossi (2006), where the elements selected were both non-linear elastic springs and linear elastic torsional spring. As mentioned by them, the non-linear elastic spring element was applied due to the lack of information about the sectional properties of carbon-carbon bond. Furthermore, the torsional spring element was used to overcome the problems with bond angles bending. They were able to simulate the three main SWNT configurations, i.e. armchair, zigzag and chiral, and graphene sheets. The geometric description of SWNT of Meo and Rossi's model was based on Cartesian equations proposed by Koloczec et al. Such approach saved considerable computational efforts during the mesh generation. Their predictions for the graphene sheets Young's modulus were in good agreement with the ones published in literature, i.e. ≈ 1.03 TPa, however, their model was limited to uniaxial tensile problems.

To overcome such problem Sun and Zhao (2005) proposed a model based on molecular-mechanics and finite element method. Sun and Zhao made usage of two types of elements. The first one was a chemical bond element which represented the intra-molecular potential energy of stretching, bending and torsional energies. This element was based on a two-node elastic rod element with an elastic joint in each end. The second element was a Lennard-Jones element which stood for the inter-molecular potential energy. In this case, a spring element with non-linear stiffness derived from the Lennard-Jones energy was applied. Sun and Zhao (2005) went further, by modifying the Morse potential function they were able to modeling the C-C chemical bond breakage. In sum, they were up of modeling stiffness and strength simultaneously. However, the data obtained, 0.4 TPa for stiffness and between 77-101 GPa for strength, were below than the usual results published in literature. A possible explanation for such behavior can be the excess of compliance introduced during stiffness matrix derivation. This hypothesis is corroborated by Pantano et al. (2004) that related the bending stiffness with the mean radius of the tube and its total wall thickness. Note that for Sun and Zhao (2005) the tensile stiffness was practically constant with the increase on nanotube diameter. The work developed by Huang et al. (2006) gave a step forward by introducing the total energy of the system expressed as a function of the location of the atomic nucleons. The same analogy between stretching and bending elements and the atoms bond were also employed. Still, they introduced a third analogy called inversion. By considering only stretching and bending, their results were similar to Sun and Zhao (2005). Tserpes and Papanikos (2005) employed beam elements in a three-dimensional (3D) space where stretching, bending, out-of-plane torsion, dihedral angle torsion and Van der Waals interactions were considered. Such model brought about results with good agreement with the literature with minimal computational efforts.

3. MOLECULAR MECHANICS FORMULATION

The molecular mechanics approach can be described by numerical methods where the equilibrium configuration of the model system is required by minimizing the energy, which consists of the sum of the interatomic potential minus any work by external forces. Dresselhaus and co-workers (1995) described SWNT in terms of the tube diameter (d) and its chiral angle (θ). The chiral vector (C_h) was defined in terms of the graphene sheet lattice translation integer indices (n, m) and the unit vectors (a_1, a_2) represented in Figure 2 and it is defined as follows:

$$\vec{C}_h = n \vec{a}_1 + m \vec{a}_2 \quad (1)$$

where the unit vectors in (x,y) coordinates are defined as:

$$\vec{a}_1 = \left(\frac{\sqrt{3}}{2}, \frac{1}{2} \right) a \quad \vec{a}_2 = \left(\frac{\sqrt{3}}{2}, -\frac{1}{2} \right) a \quad (2)$$

the length of the unit vector a is defined as 2.46 angstroms, or 1.73 times the carbon-carbon distance, i.e. 1.421 angstroms. The nanotube circumference (p) was defined by:

$$p = |C_h| = a \sqrt{n^2 + m^2 + nm} \quad (3)$$

from simple geometry, it is possible to obtain the nanotube diameter (d), as:

$$d = \frac{p}{\pi} = \frac{\sqrt{n^2 + m^2 + nm}}{\pi} a \quad (4)$$

and the chiral angle (θ), between 0 and $\pi/6$ rad, was described by Dresselhaus et al. (1995) by

$$\sin \theta = \frac{\sqrt{3}m}{2\sqrt{n^2 + nm + m^2}} \quad \cos \theta = \frac{2n + m}{2\sqrt{n^2 + nm + m^2}} \quad (5)$$

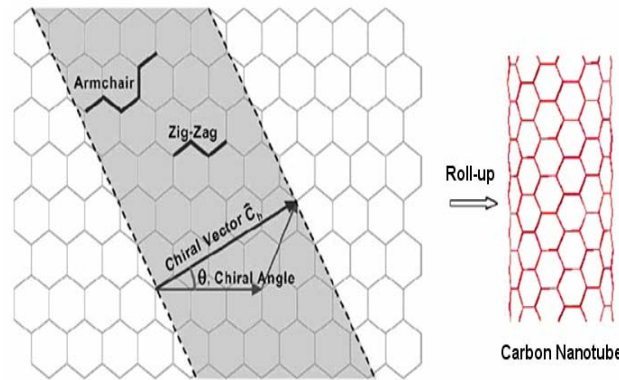


Figure 2. Chiral angle and vector representation adapted from Avila and Lacerda (2008)

The chiral indices also have a large effect on the electrical properties of CNTs. The difference of the indices of CNTs that behave like conductors, referred to as a “metallic” tubes, are always an integer, q , multiple of three, as shown

$$3q = |n - m| \text{ where } q = 0,1,2, \dots \quad (6)$$

According to Saito et al. (2005), any other index pair indicates the tube is semiconducting with an energy band gap (U_{gap}), that is proportional to a hopping parameter, ϕ , (in general 2.5-3.2 eV), as in Eq. 7.

$$U_{gap} = a \frac{\phi}{d} \quad (7)$$

In the molecular structural mechanics approach, a single-walled carbon nanotube is simulated as a space frame structure, with the covalent bonds and carbon atoms as connecting beams and joint nodes, respectively. If the beam elements simulating the covalent bonds are assumed to be of round section, then only three stiffness parameters, i.e., the tensile resistance EA , the flexural rigidity EI and the torsional stiffness GJ , need to be defined for deformation analysis. Li and Chou (2003), based on the energy equivalence between local potential energies in computational chemistry and elemental strain energies in structural mechanics, established a direct relationship between the structural mechanics parameters and the molecular mechanics force field constants. Such parameters are mathematically represented by:

$$\frac{EA}{L} = k_r \quad \frac{EI}{L} = k_\theta \quad \frac{GJ}{L} = k_\tau \quad (8)$$

where L denotes the bond length, and k_r , k_θ and k_τ are the force field constants in molecular mechanics. By assuming a circular beam cross section with diameter d , and setting the area, moment of inertia and polar moment of inertia as $A = \pi d^2/4$, $I = \pi d^4/64$ and $J = \pi d^4/32$, Tserpes and Papanikos (2005) obtained the following expressions:

$$d = 4 \sqrt{\frac{k_\theta}{k_r}} \quad E = \frac{k_r^2 L}{4\pi k_\theta} \quad G = \frac{k_r^2 k_\tau L}{8\pi k_\theta^2} \quad (9)$$

Consistent with Belytschko et al. (2002), the interatomic bonds in nanotubes are hybridized sp^2 bonds. In this paper, the interatomic potential used is a modified Morse potential function in which a bond angle-bending is added

$$E = E_{stretch} + E_{angle} \quad (10)$$

$$E_{stretch} = D_e \left\{ \left[1 - e^{-\beta(r-r_0)} \right]^2 - 1 \right\} \quad (11)$$

$$E_{angle} = \frac{1}{2} k_{\theta} (\theta - \theta_0)^2 \left[1 + k_{sextic} (\theta - \theta_0)^4 \right] \quad (12)$$

where $E_{stretch}$ is the bond energy due to bond stretch, and E_{angle} is the bond energy due to bond angle-bending, r is the length of the bond, and θ is the current angle of the adjacent bond.

Kalamkarov et al (2006) stated that at the molecular level, the interaction between individual carbon atoms can be described using the force fields of the corresponding nucleus–nucleus and electron–nucleus interaction. If electrostatic interactions are neglected, the total steric potential energy (U_{total}) which characterizes the force field can be obtained as the sum of energies due to valence (or bonded) and non-bonded interactions, given as

$$U_{total} = \sum U_R + \sum U_{\theta} + \sum U_{\phi} + \sum U_{VDW} \quad (13)$$

where U_R , U_{θ} , U_{ϕ} , and U_{VDW} correspond to energy associated with bond stretch interactions, bond angle bending, torsion (dihedral and out of plane) and Van der Waals forces (non-covalent). Figure 3 describes the interactions between atoms. A large variety of harmonic and non-harmonic potential functions have been proposed to describe the inter-atomic interactions of carbon atoms. According to Xiao and colleagues (2005), for small deformations simple harmonic approximations are enough to express the potential energy of the force fields.

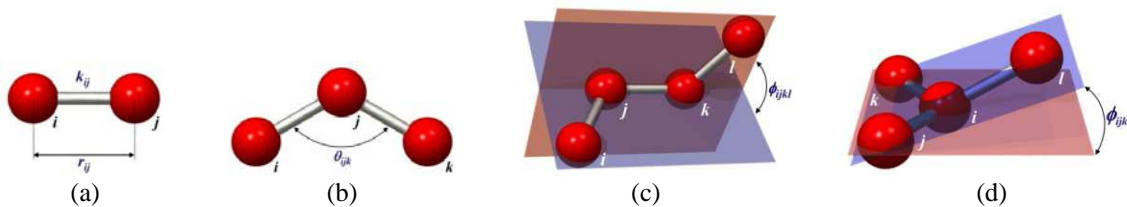


Figure 3. Covalent bonds/ interactions. (a) Stretch; (b) Bending; Torsion; (c) Dihedral; (d) Out-of-plane

Kalamkarov et al (2006) assumed that the covalent interactions between carbon atoms can be represented using simple harmonic functions. The energies associated to each covalent component of equation (13) is described as

$$U_R = \frac{1}{2} k_R (r - r_0)^2 = \frac{1}{2} k_R (\Delta r)^2 \quad (14)$$

$$U_{\theta} = \frac{1}{2} k_{\theta} (\theta - \theta_0)^2 = \frac{1}{2} k_{\theta} (\Delta \theta)^2 \quad (15)$$

$$U_{\phi} = \frac{1}{2} k_{\phi} (\phi - \phi_0)^2 = \frac{1}{2} k_{\phi} (\Delta \phi)^2 \quad (16)$$

Here, r_0 and θ_0 refer to the non-deformed interatomic distance and bond angle for a C-C bond (as it can be seen in Fig. 3). The quantities r and θ refer to the distance and bond-angle after deformation. Thus, the terms Δr , $\Delta \theta$, and $\Delta \phi$ correspond to change in bond-length, bond angle and dihedral angle, respectively. The terms k_R , k_{θ} and k_{ϕ} represent the force constants associated with stretching, bending and torsion, respectively, of the chemical bond. As stated by Li and Chou (2003), the carbon atoms in the nanotube are held together by covalent bonds of characteristic bond length and bond angles, and the corresponding molecular forces constrain any displacement of individual atoms. In the molecular structural mechanics approach, a single-walled carbon nanotube is simulated as a space frame structure, with the covalent bonds and carbon atoms as connecting beams and joint nodes, respectively. If the beam elements simulating the covalent bonds are assumed to be of round section, then only three stiffness parameters, i.e., the tensile resistance EA , the flexural rigidity EI and the torsional stiffness GJ , need to be defined for deformation analysis.

According to Ávila and Lacerda (2008), the carbon nanotubes stiffness can be predicted following the methodology described previously associated to the concept of representative volume element (RVE). Tamma and Ávila (1999) defined the RVE as the material smallest part which retains the overall material properties. When carbon nanotubes are considered, the concept of RVE has to be rearranged so that interactions between the carbon-carbon bonds and the exterior have to be considered. Ávila and Lacerda (2008) successfully rearranged the RVE concept by applying boundary conditions constraints at atomic level. A similar line of investigation was applied by Odegard et al (2002) for carbon nanotubes dispersed in a polymeric matrix. In their case, the atomic interactions polymer-carbon nanotubes were modeled by the equivalent truss model, which is similar to the model presented by Ávila and Lacerda (2008). Once the RVE is selected, the next step is to calculate the effective properties of a SWNT. Kalamkarov et al (2006) suggested to assume the nanotube be represented by an equivalent continuum tube shown in Fig. 4. By applying such strategy, the equivalent Young's modulus (E_{SWNT}) is describes as

$$E_{SWNT} = \frac{S}{\epsilon} = \frac{P/A_0}{\Delta l/l_0} \quad (17)$$

here S represents the normal stress applied to the CNT representative volume element and ϵ the correspondent strain. P is the normal force applied and Δl is the SWNT unit cell length variation due to the applied force. Finally, Kalamkarov and co-workers (2006) defined the initial CNT area A_0 as

$$A_0 = \pi \left[\left(\frac{d}{2} + \frac{t}{2} \right)^2 - \left(\frac{d}{2} - \frac{t}{2} \right)^2 \right] \quad (18)$$

where d is the nanotube diameter and t its wall thickness. Using the same principle applied to Young's modulus, it is possible to establish a mathematical expression for shear modulus. The carbon nanotube effective shear modulus (G_{SWNT}) is given by

$$G_{SWNT} = \frac{Tl_0}{\alpha J_0} \quad (19)$$

here T is the moment of torsion applied to the SWNT unit cell (also called as RVE), α is the torsion angle applied to the SWNT unit cell, while the moment polar moment of inertia (J_0) is represented by

$$J_0 = \frac{\pi}{2} \left[\left(\frac{d}{2} + \frac{t}{2} \right)^4 - \left(\frac{d}{2} - \frac{t}{2} \right)^4 \right] \quad (20)$$

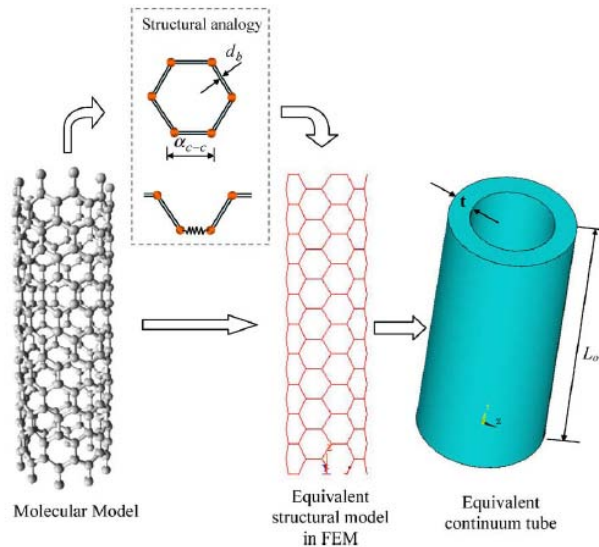


Figure 4: Equivalence of molecular, finite element and continuum model from Kalamkarov et al (2006)

4. DATA ANALYSIS

Following Belytschko et al. (2002), Li and Chou (2003) the numerical simulations will be performed at 0K. The carbon-carbon bonds are simulated by a beam element with six degrees-of-freedom (DOF), i.e. three translations and three rotations as suggested by Tserpes and Papanikos (2005). To be able to generate each group of SWNT, i.e. armchair, zigzag and chiral a macro subroutine was developed and implemented into a commercial finite element commercial code named ANSYS V.11. In the present model, the equivalent values for the three major stiffness constants, which are $k_r = 6.52E-7 \text{ Nnm/rad}$, $k_\theta = 8.76E-10 \text{ Nnm/rad}^2$ and $k_\tau = 2.78E-10 \text{ Nnm/rad}^2$, were obtained from Li and Chou (2003). The remaining parameters from equations 8 to 10 were from Belytschko et al. (2002). They defined the C-C bond radius as $1.421E-10 \text{ m}$, while $D_o = 6.03105E-19 \text{ Nm}$, $\beta = 2.625E-10 \text{ 1/m}$. The initial angular deflection was defined by them as $\theta_o = 2.094 \text{ rad}$ and $k_{\text{sextic}} = 0.754 \text{ rad}^4$.

The boundary conditions impositions are similar to load cases I and II described by Odegard and co-workers (2002) and are described in details in Ávila and Lacerda (2008). First, sub marginal nodes on one side of the generated nanotube were completely constrained, and then a prescribed displacement on axial direction was imposed on the nodes on the other side of the SWNT. Note that varying boundary conditions from imposing restrictions on axial

directions only to constraining all degrees-of-freedom do not have significant effect on reaction forces or nanotube deformation for the range of lengths used.

As described by Ávila and Lacerda (2008), the representative volume element (RVE) assumes different formats due to SWNT configuration. To be more specific: the (4,2) chiral configuration was represented by 112 atoms and 162 C-C bonds, while for the (17,9) chiral format the number of atoms and C-C bonds were 623 and 908, respectively. These changes are the main reason for differences on RVE total length. It is worth to mention that each atom corresponds, into molecular mechanics model, to a node with six degrees-of-freedom, i.e., three displacements and three rotations. Furthermore, the carbon-carbon bond is represented by a beam element with two nodes, one in each end. The three groups of SWNT were investigated, i.e. armchair (8,8), zigzag (14,0) and chiral (11,5). The idea here is to get as input data the wall thickness applied for each of the benchmark research selected, and compared the present model predictions using the input data with the results presented by the corresponding authors. Table 1 reviews all data obtained and the benchmark ones.

Table 1. Comparative study on wall thickness effect on stiffness (Young's modulus – E)

Authors	Wall thickness [nm]	E [TPa]	Model prediction		
			Armchair (8,8)	Zigzag (14,0)	Chiral (11,5)
Yakobson et al	0.066	5.5	5.282	5.298	4.962
Hernandez et al	0.34	1.24	1.025	1.028	0.963
Pantano et al	0.075	4.84	4.648	4.662	4.367
Lu	0.34	0.974	1.025	1.028	0.963
Odegard et al	0.69	0.496	0.505	0.507	0.475
Li and Chou [†]	0.34	1.01	1.025	1.028	0.963
Tserpes and Papanikos [†]	0.147	2.395	2.377	2.385	2.423
Ávila and Lacerda [†]	0.34	1.005	1.025	1.028	0.963

[†]Young's modulus (E) is the mean value of these author's predictions

There is no doubt that carbon nanotube wall thickness has influence on overall stiffness. When the present model is compared against the three major groups of simulation methods, i.e., molecular dynamics, continuum mechanics and molecular mechanics, some conclusions can be drawn. The lower and upper bounds of the molecular dynamics predictions are obtained with chiral configuration. The largest difference (28.76%), named upper bound, can be explained when the tight binding model is analyzed. Hernandez et al (1998) did not consider the "atoms rotations", in other words, for them stiffness was calculated taking the nanotube strain energy regardless the chiral angle. The molecular dynamics simulations performed by Yakobson et al (1996) lead to the lower bound difference (10.84%). Note that Yakobson and his collaborators considered the nanotube behavior beyond the nonlinear instability. By performing the MD simulation including buckling their model was capable of identifies with accuracy the shell energy strain. Notice that carbon nanotubes are essentially long shell columns. The continuum mechanics based models appeared to be more accurate, as the difference lower and upper bounds are between the 1.14% and 10.84% range. These models are essentially closer to the molecular mechanics approached used in this research. To be more specific, in Lu (1997), for instance, although in the empirical force-constant model, the atomic interactions near the equilibrium structure are approximated by the sum of pair wise harmonic potentials between atoms, the elastic constants are calculated from the second derivatives of the energy density with respect to various strains. Still, the Young's modulus was calculated by Lu (1997) using the traditional second derivative of the strain energy density with respect to the axial strain. However, Lu's model has a weakness; the empirical force-constant model is insensible to the chiral angle atoms rotation. His model is not able to distinct the differences in terms of atoms location and consequently shell configuration. As expected the models based on molecular mechanics approach provided the smaller differences between proposed model and the three benchmark models, i.e., Ávila and Lacerda (2008) and Tserpes and Papanikos (2005). Again the largest difference was noticed on chiral condition is due to boundary conditions.

Another important conclusion is that larger walls lead to smaller Young's modulus. Such hypothesis can be corroborated by Odegard and co-workers (2002) that, based on equivalent-continuum model, stated that Young's modulus is inversely proportional to SWNT cross sectional area. Additionally, Li and Chou (2003) attributed the variation among the three configurations to small differences on radius. Tserpes and Papanikos (2005), however, also called the attention to the chirality effect. According to them, the diameter effect is more evident on armchair and zigzag configurations, while the chiral form is less affected. Notice that as the nanotube diameter becomes smaller than 1 nm the curvature effect described by Li and Chou (2003) is more evident. Furthermore, as demonstrated by Fig. 5A, as the nanotube diameter increases the Young's modulus has an asymptotic behavior close to the graphene sheet. When the shear moduli are analyzed the same trend is observed. As it can be seen in Fig. 5B, the shear modulus is sensitive to both diameter and chirality, especially at small diameters (less than 1.5 nm). This sensitivity is due to the effect of curvature, which is a function of tube diameter.

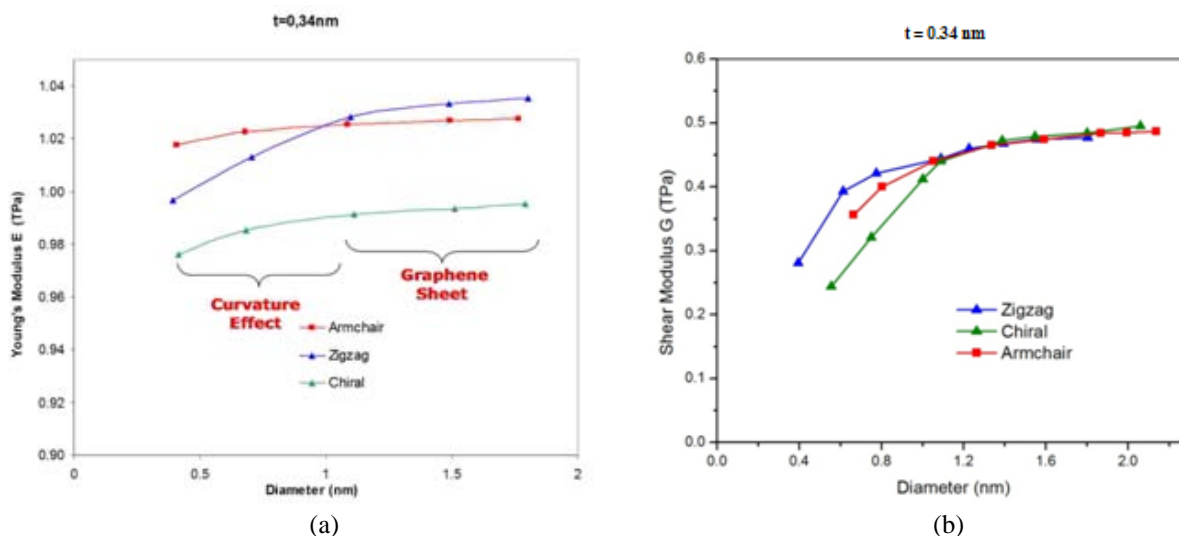


Figure 5. CNT stiffness variation. (a) Young's modulus; (b) Shear modulus

A small nanotube diameter leads to large curvature and distortion of the carbon-carbon (C-C) bonds. This phenomenon brings as a consequence a large elongation (Δh) of the nanotube. As diameter increases, the effect of curvature diminish and the Young's modulus of SWNT's approaches that of graphene sheet (1.1 TPa) when considering 0.34 nm as the wall thickness, for which no effect of curvature is present. As the SWNT is modeled as a three-dimensional tubular structure, the Poisson effect is an important issue. Fig 6A represents the Poisson's ratio as a function of the nanotube radius. As it can be observed, in all configurations, the Poisson ratio seems to seek an asymptotic value as the radius gets larger.

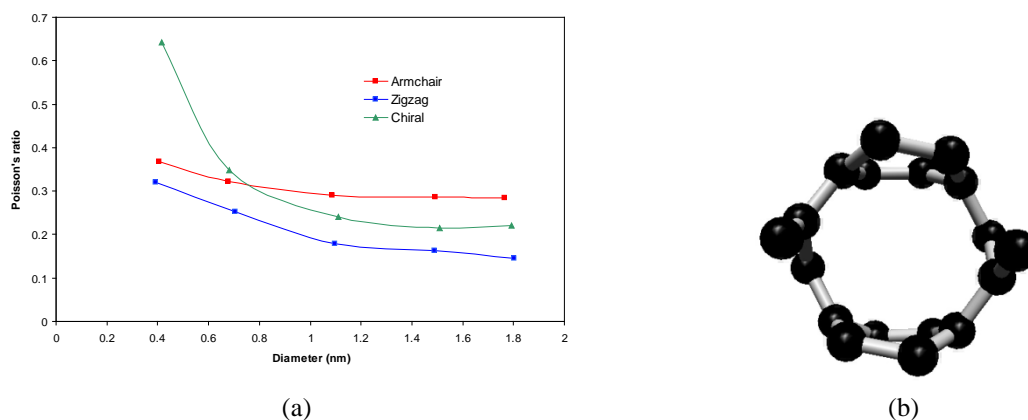


Figure 6. Poisson's ratio. (a) Distribution as function of nanotube diameter; (b) CNT unit cell

The Poisson ratio values obtained are between 0.28 and 0.36 for armchair, 0.15 and 0.31 for zigzag, while for the chiral configuration the values are between 0.22 and 0.66. The results reported by Salvat-Delmont and Rubio (2002) for nanotubes with diameter larger than 1 nm are between 0.16, 0.19 and 0.18, for armchair, zigzag and chiral, respectively. The difference between the present model and the results supplied by Salvat-Delmont and Rubio (2002) can be attributed to their model uncertainties and the boundary conditions applied. They also mentioned that their results can be differing of at least $\pm 10\%$. When the results are compared against MD simulations performed by Xiao et al (2005), all three configurations are in good agreement for larger radius. Lu (1997) reported Poisson values between 0.26 and 0.32 for diameters larger than 1 nm. Sun and Zhao (2003), however, applying the finite element approach in a armchair configuration for 0.8 nm diameter obtained a 0.35 Poisson ratio, while a nanotube with 2.8 nm diameter lead to a 0.31 Poisson ratio. Notice that for this case the present model is in good agreement with those results reported by Sun and Zhao.

Natsuki et al (2004) also calculated the Poisson ratio of single-walled carbon nanotubes. His model was based on analytical model using a three-dimensional grid associated to springs. He described, for the armchair configuration, values between 0.27-0.29 when the nanotube diameter varied between 0.5-2.5 nm. For the zigzag configuration, the Natsuki's results ranged from 0.27-0.33 for the same range of diameter. No values for the chiral configuration were reported. Even though, a comparison between the present model and the Natsuki's lead to the same conclusion, the

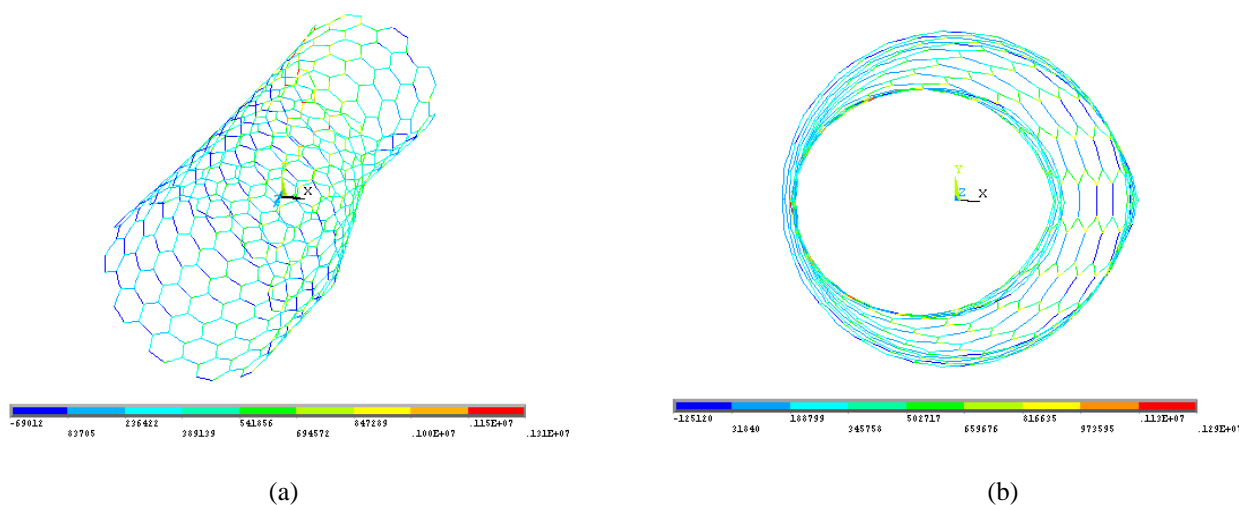
results seems to be in good agreement. From the Poisson ratio variability listed in literature, it is possible to infer that Poisson's ratio can be represented between 0.15 and 0.29. Those values are dependent of nanotube diameter. The results presented by Popov and Van Doren (2000) also corroborate the model's data. Their model based on analytical expression for the velocity of the longitudinal and torsional sound waves in SWNT leads to an asymptotic value of Poisson's ratio of 0.21. However, one final result has to be analyzed, the Poisson's ratio of 0.64. One possible explanation for such result is the CNT geometry. This data corresponds to the chiral (4,2) configuration. From Fig 6B, it is possible to observe that for this configuration, the transverse section is not hexagonal but pentagonal. Such geometry leads to a much larger axial strain which has direct influence into Poisson's ratio.

Once the model has been validated, the next step is the investigation of hetero-junctions. According to Terrones (2003), hetero-junctions have been attracting much attention due to their differences into electrical properties. However, as mentioned by Liu and co-workers (2004), mechanical properties are also affected by these geometric and atomic changes. Furthermore, they also called the attention for the absence of some carbon atoms leading to the presence of heptagons and/or pentagons into the nanotubes structures. As we are analyzing three types of SWNTs and they can be combined in pairs, there are six possible combinations. Table 2 summarizes these combinations. To be able to compare the stress distribution in all defect configurations, the same axial strain was imposed in all cases, i.e. 1%. As recognized by Belytschko et al (2002), this axial strain imposed in this paper is inside the elastic range. Our objective here is to identify points with high probability of failure.

Table 2. CNTs hetero-junctions generated during the simulations

Case	Nanotubes	Hetero-junction	Normalized Normal Stress
I	Armchair(8,8) + Armchair (11,11)	Sadoc	1.31
II	Zigzag (14,0) + Zigzag (19,0)	Sadoc	1.29
III	Chiral (11,5) + Chiral (14,8)	Sadoc	1.51
IV	Armchair (8,8) + Zigzag (14,0)	Dunlap	1.11
V	Chiral(11,5) + Armchair (8,8)	Dunlap	1.29
VI	Chiral(11,5) + Zigzag (14,0)	Dunlap	1.19

By observing Figures 7A-F, some conclusions can be drawn. In all three cases, i.e. I, II and III, the highest stress occurred on the opposite side of the defect. Notice that the defect side is the one with pentagons and heptagons. This phenomenon can be explained by the defect geometry itself. The curvature on the defect side leads to a more flexible structure. This bendy behavior brings a stress field with lower values on this side. As the system must be equilibrium, the opposite side gets higher stresses. Case III presents a peak stress 14% higher than the two orders. The reason for this increase on peak stress can be the atoms rotations on chiral configuration. Perceive that the Dunlap defect behavior is completely different than the Sadoc type analyzed previously. Under tensile loading the Dunlap defect heads for a straight line condition. As noticed in Figs. 7D-7F, the highest stress locus is on Dunlap's internal side, which has the smaller curvature radius. As described by Ávila and Lacerda, this small curvature radius guides to larger stresses.



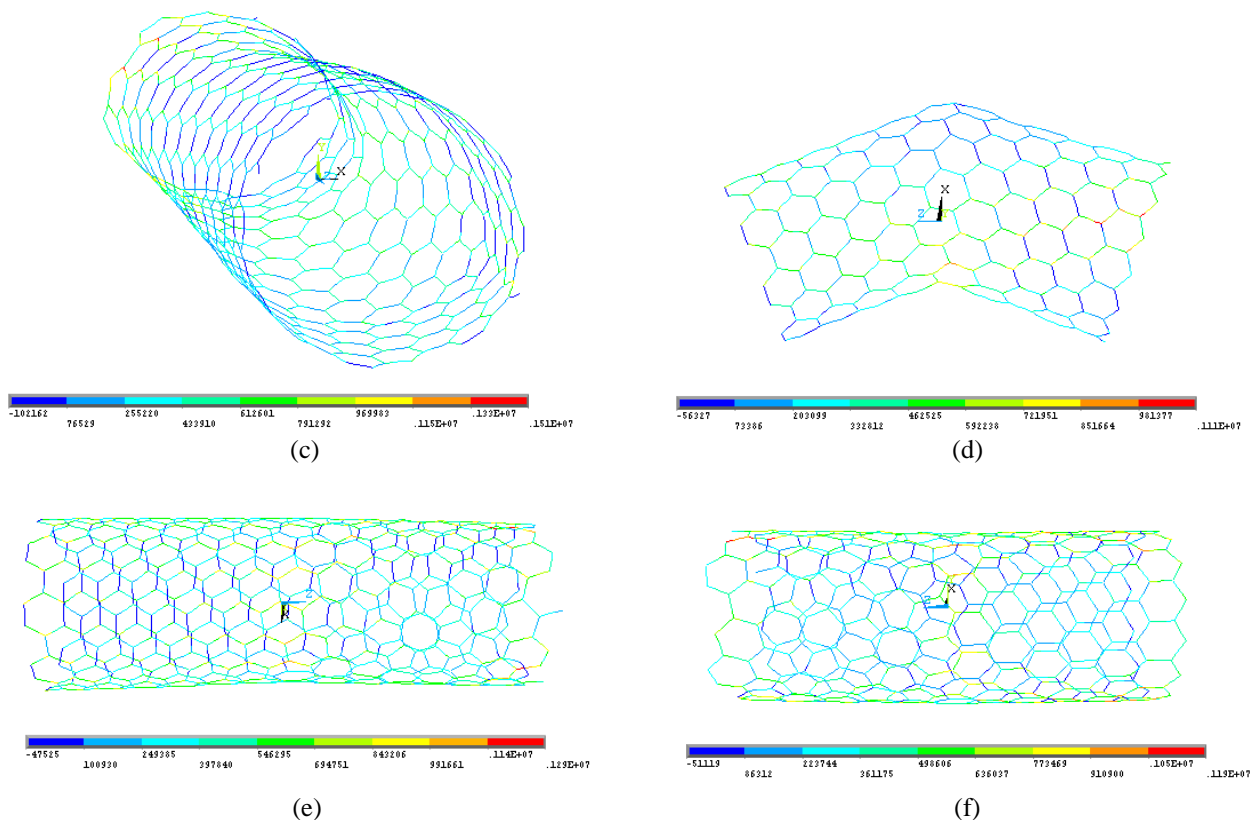


Figure 7. Hetero-junction normalized stress distribution

5. CLOSING COMMENTS

A molecular mechanics model for armchair, zigzag and chiral single-walled carbon nanotubes has been implemented. The molecular structural mechanics approach was employed to exam the effect of wall thickness, diameter and chirality's effect on SWNT stiffness. Results suggested that stiffness (Young's modulus) is inversely proportional to wall thickness. Moreover, the curvature effect due to SWNT radius has also an effect on stiffness. Smaller radius conducts to larger curvatures and elongations. Meanwhile, on SWNT with large radius, the curvature effect is negligible and Young's modulus approaches 1.0 TPa. The SWNT configuration less affected by the radius/curvature variations seems to be the chiral one due to its complex geometry. The SWNT unit cell stress distributions also revealed critical regions where the failure is most likely to occur. For armchair case, it seems to be the bond angle variation region, while for the zigzag case the dihedral angle torsion region is the critical one. The chiral case guide to different locations of high stresses concentration as a function of the atoms location.

The SWNT configuration less affected by the radius/curvature variations seems to be the chiral one due to its complex geometry. The SWNT unit cell stress distributions also revealed critical regions where the failure is most likely to occur. For armchair case, it seems to be the bond angle variation region, while for the zigzag case the dihedral angle torsion region is the critical one. The chiral case guide to different locations of high stresses concentration as a function of the atoms location. The Poisson's ratio of SWNT was also simulated and the results were between 0.15-0.29. Notice that nanotube radius variations also affect the Poisson's ratio. Again the chiral configuration seems to be the most sensible to radius variations.

Two types of CNTs hetero-junctions were simulated, i.e. Sadoc and Dunlap. By applying a prescribed axial displacement, we were able to locate the highest stress concentration region. From all six configurations studied, the one with highest normalized normal stress is the Sadoc type from chiral-chiral arrangement. By applying this strategy, it was possible to identify the locus if highest probability of failure for each configuration. The numerical simulations have good agreement with experimental data provided by Hernandez and Yakobson. Furthermore, data from numerical simulations provided by Pantano and Chou are also in good agreement with the present model.

6. ACKNOWLEDGEMENTS

The authors would like to acknowledge the financial support provided by the Brazilian Research Council (CNPq) Grants 470511/2006-0, 472213/2007-5 and 300434/2008-1.

7. REFERENCES

- Ávila, A.F., & Lacerda G.S.R., 2008. Molecular Mechanics Applied to Single-walled Carbon Nanotubes. *Materials Research: Ibero American Materials Journal*, vol. 11, pp. 239-247.
- Belytschko, T., Xiao, S.P., Schats, G.C., & Ruoff, R.S., 2002, "Atomistic Simulations of Nanotube Fracture". *Physics Review B*, vol. 65, pp. 2354301-2354308.
- Dresselhaus, M.S., Dresselhaus, G., & Saito, R., 1995, "Physics of Carbon Nanotubes". *Carbon*, vol. 33, n. 7, pp. 883-891.
- Gates, T.S., Odegard, G.M., Frankland, S.J.V., Clancy, T.C., 2005, "Computational Materials: Multi-Sscale Modeling and Simulation of Nanostructured Materials". *Composites Science and Technology*, vol. 65, n. 15, pp. 2416-2434.
- Hernandez, E., Goze, C., Bernier, P., & Rubio, A., 1998, "Elastic Properties of C and BxCyNz Composite Nanotubes". *Physical Review Letters*, vol. 80, n. 20, pp. 4502-4505.
- Huang, M-Y., Chen, H-B., Lu, J-N., & Zhang, P-Q., 2006, "A Modified Molecular Structural Mechanics Method for Analysis of Carbon Nanotubes". *Chinese Journal of Chemical Physics*, vol. 19, n.4, pp. 286-290.
- Iijima S., 1991, "Helical Microtubes of Graphitic Carbon". *Nature*, vol. 354, pp. 56-58.
- Jin, Y., & Yuan, F.G., 2003, "Simulation of Elastic Properties of Single-Walled Carbon Nanotubes", *Composites Science and Technology*, vol. 63, n. 8, pp. 1507-1515.
- Kalamkarov, A.L., Georgiades, A.V., Rokkam, S.K., Veedu, V.P., & Ghasemi-Nejhad, M.N., 2006, "Analytical and Numerical Techniques to Predict Carbon Nanotubes Properties". *International Journal of Solids and Structures*, vol.43, n. 20, pp. 6832-6854.
- Krishnan, A., Dujardin, E., Ebbesen, T.W., Yianilos, P.N., & Treacy, M.M.J., 1998, "Young's Modulus of Single-Walled Nanotubes". *Physics Review B*, vol. 58, n. 20, pp. 4013-4019.
- Li, C., & Chou, T-W., 2003, "A Structural Mechanics Approach for the Analysis of Carbon Nanotubes". *International Journal of Solids and Structures*, vol. 40, n. 10, pp. 2487-2499.
- Liu, W.K., Karpov, E.G., Zhang, S., & Park, H.S., 2004, "An Introduction to Computational Nanomechanics and Materials". *Computer Methods and Applied Mechanics in Engineering*, vol. 193, n. 10, pp. 1529-1578.
- Lourie, O., & Wagner, H.D., 1998, "Evaluation of Young's Modulus of Carbon Nanotubes by Micro-Raman Spectroscopy". *Journal of Materials Research*, vol. 13, n. 20, pp. 2418-2422.
- Lu, J.P., 1997, "Elastic Properties of Carbon Nanotubes and Nanoropes". *Physics Review Letters*, vol. 79, n. 7, pp. 1297-1300.
- Melchor, S., & Dobado, J.A., 2004, "CoNTub: An Algorithm for Connecting Two Arbitrary Carbon Nanotubes". *Journal of Chemical Information and Computer Science*, Vol 44, pp. 1639-1646.
- Meo, M., & Rossi, M., 2006, "Prediction of Young's Modulus of Single Wall Carbon Nanotubes by Molecular-Mechanics Based Finite Element Method". *Composites Science and Technology*, vol.66, n. 10, pp. 1597-1605.
- Natsuki, T., Tantrankarn, K., & Endo, M., 2004, "Effects of Carbon Nanotube Structures on Mechanical Properties". *Applied Physics A: Materials Science and Processing*, vol. 79, n. 1, pp. 117-124.
- Odegard, G.M., Gates, T.S., Nicholson, L.N., & Wise, K.E., 2002, "Equivalent Continuum Modeling of Nano-Structured Materials". *Composites Science and Technology*, vol. 62, n. 10, pp. 1869-1880.
- Odegard, G.M., Frankland, S.J.V., & Gates, T.S., 2005, "Effect of Nanotube Functionalization on the Elastic Properties of Polyethylene Nanotube Composites", *AIAA Journal*, vol. 43, n. 8, pp. 1828-1835.
- Pantano, A., Parks, D.M., & Boyce, M.C., 2004, "Mechanics of Deformation of Single- and Multi-Wall Carbon Nanotubes". *Journal of the Mechanics and Physics of Solids*, vol. 52, n. 6, pp. 789-821.
- Popov, V.N., & Van Doren, V.E., 2000, "Elastic Properties of Single-Walled Carbon Nanotubes". *Physical Review B*, vol. 61, n.4, pp. 3078-3084.
- Salvatat-Delmont, J.P.; Rubio, A., 2002, "Mechanical Properties of Carbon Nanotubes: A Fiber Digest for Beginners". *Carbon*, vol. 40, n. 10, pp. 1729-1734.
- Saito, R., Dresselhaus, G., & Dresselhaus, M.S., 2005, *Physical Properties of Carbon Nanotubes*. Imperial College Press.
- Sun, X., & Zhao, W., 2005, "Prediction of Stiffness and Strength of Single-Walled Carbon Nanotubes by Molecular Mechanics Based Finite Element Method". *Materials Science and Engineering A*, vol. 390, n. 3, pp. 366-371.
- Tamma, K.K., & Ávila, A.F., 1999, "An integrated micro/macro modeling and computational methodology for high temperature composites". In: *Thermal Stress V*, Hetnarski, R. ed., Lastran Corporation, pp. 143-256.
- Terrones, M. 2003, "Science and Technology of the Twenty-First Century: Synthesis, Properties, and Applications of Carbon Nanotubes". *Annual Review of Materials Research*, vol. 33, pp. 419-501.
- Tserpes, K.I., & Papanikos, P., 2005, "Finite Element Modeling of Single-Walled Carbon Nanotubes". *Composites Part B*, vol. 36, n.4, pp. 468-477.
- Wang, Y., Sun, C., Sun, X., Hinkley, J., Odegard, G.M., & Gates, T.S., 2003, "2-D Nano-Scale Finite Element Analysis of Polymer Field". *Composites Science and Technology*, vol. 63, pp. 1581-1590.

- Xiao, J.R., Gama, B.A., & Gillespie Jr., J.W., 2005, "An Analytical Molecular Structural Mechanics Model for the Mechanical Properties of Carbon Nanotubes". *International Journal of Solids and Structures*, vol. 42, n. 24, pp. 3075-3092.
- Yakobson, B.I., Bradec, C.J., & Bernholc, J., 1996, "Nanomechanics of Carbon Tubes: Instabilities Beyond Linear Range". *Physical Review Letters*, vol. 76, n. 20, pp. 2511-2514.
- Yu, M.F., Lourie, O., Dyer, M.J., Moloni, K., Kelly, T.F., & Ruoff, R.S., 2000, "Strength and Breaking Mechanics of Multiwalled Carbon Nanotubes under Tensile Load". *Science*, vol. 287, pp. 637-640.

8. RESPONSIBILITY NOTICE

The first author is the only responsible for the printed material included in this paper.